Multiscaling in an *YX* model of networks

Petter Holme,[1,2] Zhi-Xi Wu,[1] and Petter Minnhagen[1]
[1]*Department of Physics, Umeå University, 901 87 Umeå, Sweden*
[2]*Department of Energy Science, Sungkyunkwan University, Suwon 440-746, Korea*
(Received 2 June 2009; revised manuscript received 4 August 2009; published 29 September 2009)

We investigate a Hamiltonian model of networks. The model is a mirror formulation of the *XY* model (hence the name)—instead of letting the *XY* spins vary, keeping the coupling topology static, we keep the spins conserved and sample different underlying networks. Our numerical simulations show complex scaling behaviors with various exponents as the system grows and temperature approaches zero, but no finite-temperature universal critical behavior. The ground-state and low-order excitations for sparse, finite graphs are a fragmented set of isolated network clusters. Configurations of higher energy are typically more connected. The connected networks of lowest energy are stretched out giving the network large average distances. For the finite sizes we investigate, there are three regions—a low-energy regime of fragmented networks, an intermediate regime of stretched-out networks, and a high-energy regime of compact, disordered topologies. Scaling up the system size, the borders between these regimes approach zero temperature algebraically, but different network-structural quantities approach their $T=0$ values with different exponents. We argue this is a, perhaps rare, example of a statistical-physics model where finite sizes show a more interesting behavior than the thermodynamic limit.

DOI: 10.1103/PhysRevE.80.036120 PACS number(s): 89.75.Da, 64.60.aq, 64.60.an, 87.23.Ge

I. INTRODUCTION

The *XY* model is one of the classical and most versatile spin models of statistical mechanics. It has been used in many physical contexts, from superconductors [1] to lattice gauge theory of quantum chromodynamics [2], and furthermore applied to emergent phenomena in systems such as bird flocks [3] and parallel discrete-time simulations [4]. In general, the *XY* model describes a system of N pairwise interacting units. Let the interaction be represented by a graph $G=(V,E)$, where V is the set of units, or vertices, and E is the set of *edges* (pairs of coupled units). Each unit $i \in V$ is characterized by a real number θ_i called the *spin* of i. The probability of a certain combination G and $\{\theta_i\}_{i \in V}$ is proportional to $\exp(-H/T)$, where the parameter T is called temperature (parametrizing the disorder of the system) and H is the (ferromagnetic) Hamiltonian

$$H = -\sum_{(i,j) \in E} \cos(\theta_i - \theta_j), \tag{1}$$

a function that in physical systems represents the energy of a configuration. (Note that, in our formalism, temperature and energy are dimensionless.) From the symmetry of the cosine function in Eq. (1), we see that the values of θ_i only matter modulo 2π. For this reason θ_i is commonly restricted to the interval $(0,2\pi]$.

Traditionally, studies of the *XY* model take G as a lattice graph—a graph that can be drawn as a lattice (a discrete subgroup spanning the vector space $\mathbb{R}^d$, where d is the dimension, a natural number)—and considered fixed, while $\{\theta_i\}_{i \in V}$ is the object of study. (The most important result is perhaps that for a two-dimensional lattice structure, the *XY* model undergoes a peculiar phase transition, the Kosterlitz-Thouless transition [5] between a disordered phase and a phase with algebraic spin correlations.) Sometimes random graph ensembles are used [6–8], sometimes regular topologies that are not mathematical lattices [9], but usually G is static (the only exception we are aware of is Ref. [10], where the *XY* model is simulated on a graph being rewired without any bias). In this paper, we turn the situation around—we fix $\{\theta_i\}_{i \in V}$ and let G be only restricted by the number of vertices N, the number of edges M, and that the graph is simple (i.e., that there are no multiple edges or self-edges). The spins are, like common practice when initializing the *XY* model for Monte Carlo simulations, drawn with uniform probability. Our model is a conceptual mirror image of the *XY* model—hence we call it the *YX* model.

The *YX* model defines an ensemble of graphs and is thus more related to the recent works on phenomenological models of complex networks [11–13]. Authors have studied general classes of graphs sampled with a Boltzmann-like probability—so-called exponential random graphs [14], Markov graphs [15], p-star models [16], or statistical-mechanics models [17] depending on the background of the author. These models are used for sampling networks with some prescribed structures; they are thus not microscopic, or mechanistic, models and usually not analyzed in terms of emergent properties in the $N \to \infty$ ("thermodynamic") limit. Our *YX* model is also related to hidden-variable models [18–20] where some variables (in this case θ_i) assigned to the vertices are affecting their position in the network. These classes of models form a framework for modeling several types of social networks. Assume at first that opinions (or some other psychological or behavioral trait) of individuals can be represented, or approximated, as a spin. (The model can be generalized straightforwardly to traits represented as binary [21] or multidimensional [22] variables.) Many forms of social networks are shaped by a homophily between the individuals—if the two individuals have similar traits, they are more likely to be attached by an edge [23]. The third assumption is that the social ties evolve faster than the opinions (as in models of social segregation [24] or in some limits of coevolution models of networks and opinions

[25,26]). Our model is a simple model generating networks whose growth is governed by these factors, with the temperature parametrizing the strength of the homophily. We will present and analyze it as an equilibrium statistical-mechanics model, but it could be extended to a dynamic model straightforwardly (easiest, perhaps, by modeling the time evolution by METROPOLIS Monte Carlo sampling [27]). Another application of our model is corporate network. Both networks of firms are connected if they trade with each other [28] and if their shares (or other financial instruments) are correlated in time [29]. We have pointed out the versatility of both the *XY* model and the related network models; we believe our proposed model have yet more applications. In the rest of the paper, we will present the simulation scheme in more details and analyze the size scaling of network-structural quantities.

II. SIMULATIONS

We simulate our *YX* model using METROPOLIS Monte Carlo sampling [27]. For one update *step*, we choose three distinct vertices i, j, and k such that $(i,j) \in E$ but $(i,k) \notin E$ at random. Let E' be E with (i,j) replaced by (i,k), then we accept the change (replacing E by E') if $H(E) \geq H(E')$ or if $H(E) < H(E')$, with a probability proportional to

$$\exp\left(\frac{H(E) - H(E')}{T}\right). \tag{2}$$

Let, furthermore, N such trial steps (where one edge is considered for rewiring) comprise one *sweep*.

The configuration space of our *YX* model is, as will be discussed later, probably not very rugged. Still, to be on the safe side, we use the exchange Monte Carlo method [30] capable of, even for glassy systems with many local energy minima, sampling the configuration space evenly in a limited time. In exchange Monte Carlo, an even number of systems is simulated in parallel for a sequence of temperatures. After some intervals, with a probability dependent on the current configuration, two systems at adjacent temperatures are exchanged so that one system moves up in temperature, the other one down. In our simulations, we test for an exchange every 10^5th sweep. We measure network quantities with the same frequency as the tests for exchanges. Before we start measuring, we run 10^7 sweeps for the system to reach equilibrium (which is roughly 10 times longer than it takes for all quantities for all sizes and temperatures to converge). We use 100 measurements to calculate intermediate averages. This procedure is then repeated for 100 random initial conditions and the averages and standard errors of the intermediate averages are the values we present below.

Unless otherwise stated, we will use $M=2N$ (the edge density of a two-dimensional square lattice). We chose an exponential set of 20 temperatures per system size selected in a preliminary study to capture the most interesting region.

III. NUMERICAL RESULTS

A. Low-energy configurations

What is the ground-state configuration of the *YX* model? First consider a simpler example—suppose N is a multiple of 3, $N=M$, and the angles $\{\theta_i\}_{i \in V}$ are evenly spread out over the circle, i.e., $\theta_i = 2\pi i/N$. The minimal distance between any pair of θ_i is the distance $2\pi/N$ between two adjacent vertices along the circle. There are exact M such pairs, so the ground state is $E=\{(1,2),(2,3),\ldots,(N-1,N),(N,1)\}$. Let $f=M+H$ measure how far from the lowest energy of a model, where $\{\theta_i\}_{i \in V}$ is unconstrained, the configuration is (similar to "frustration" in antiferromagnetic spin systems and spin glasses). For the state of circularly coupled edges, we have (by Taylor expansion, $\cos\phi \approx 1-\phi^2/2$ for small ϕ) $f=M-M\cos(2\pi/N) \approx 2M\pi^2/N^2 = 2\pi^2/N$ for large N. Another low-energy configuration would be to couple nearby vertices into $N/3$ triangles—$E=\{(1,2),(2,3),(3,1),\ldots,(N-2,N-1),(N-1,N),(N,N-2)\}$. f is in this case twice as large as in the circular configuration. If we change the system above, so $\theta_1 = 2\pi/N + \delta_\theta$ (for some small perturbation $0 < \delta_\theta < \pi/N$) and the rest is the same, then the f increases with δ_θ^2 for the circular configuration, while it decreases by $6\pi^2\delta_\theta/N - \delta_\theta^2$ for the configuration of isolated triangles. This example can be fairly straightforwardly generalized to higher edge densities. It suggests that fragmented configurations benefit from an irregular distribution of angles, while circular distributions should give the lowest energies at evenly distributed angles. Since we sample $N^{-\epsilon}$ by uniform randomness, in the $N \to \infty$ limit, the ground state should be a circulant (a graph where vertices are connected to their nearest neighbors on a circle). The fragmented states can utilize the gaps in the distribution of drawn θ_i values by omitting edges across such gaps. For finite sizes, it could happen that the ground state is fragmented rather than a circulant. Indeed, this is what we see in our simulations.

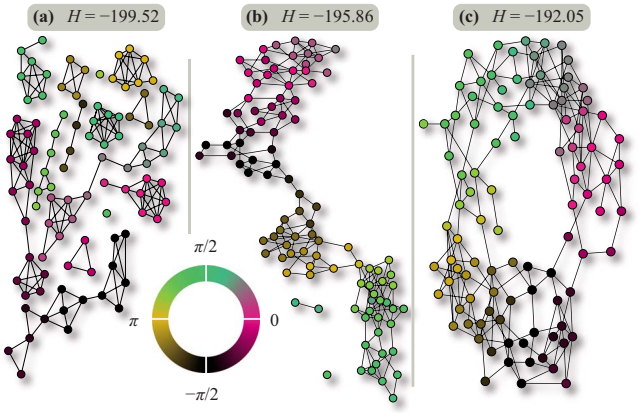

FIG. 1. (Color online) Three low-energy configurations of our *YX* model with 100 vertices.

In Fig. 1, we show three low-energy configurations for a small system size. The lowest energy state, with $f=0.48$, is fragmented; the other two, with $f=4.14$ and 7.95, are more elongated, closer to circulants. As we will see, for finite sizes, fragmented states such as Fig. 1(a) have the lowest energies while the circulants have larger entropies, making configurations such as Figs. 1(b) and 1(c) dominant at higher temperatures. In the large temperature limit, the networks are Erdős-Rényi random graphs [11–13].

B. Cluster sizes

Now we turn to the quantitative results. In Fig. 2, we plot the relative fraction of the vertices not a part in the largest

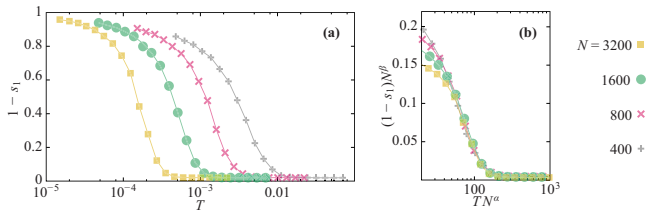

FIG. 2. (Color online) The fraction of vertices not part of the largest connected cluster. In (a), we show the raw data as a function of temperature for four different system sizes. In (b), we determine the scaling exponents for low temperatures to $\alpha=1.61\pm0.05$ and $\beta=0.22\pm0.03$. Standard errors are smaller than the symbol size and omitted for clarity. Lines are guides for the eyes.

cluster, $1-s_1$. Compared to spin models such as the *XY* model, the temperatures where the interesting behavior occurs are much lower. The interesting behavior—the fragmentation of the network—is best monitored in a logarithmic temperature scale. The onset of fragmentation approaches zero (as expected from the discussion above) as the system size increases. In Fig. 2(b), we show that for $\alpha=1.61\pm0.05$ and $\beta=0.22\pm0.03$, we have

$$1-s_1 \approx N^{-\beta}F_+(TN^{\alpha}) \tag{3}$$

for a smooth function F and $TN^{1.61}\gtrsim 80$. The onset of fragmentation thus moves to zero such as $N^{-\alpha}$. Note that this scaling relation is itself not indicative of critical behavior in the rescaled temperature TN^{α}. We observe that the scaling region is larger for smaller rather than larger system sizes, which is also not supporting an emergent critical behavior in s_1.

An unexpected phenomenon in the *YX* model is that there seems to be no universality in this size scaling of the network-structural quantities. An example of this is seen in Fig. 3 where we plot the temperature dependence of the relative size of the second-largest component s_2. In many systems with a fragmentation phase transition, such as percolation or network models of segregation [25,26], s_2 or s_2/s_1 can be used to characterize the critical behavior. Also in our

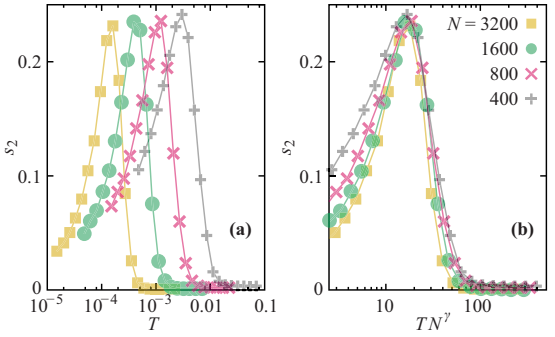

FIG. 3. (Color online) The fraction of the second-largest cluster. (a) displays the raw data of s_2 as a function of temperature. In (b), we determine the scaling factor $\gamma=1.44\pm0.02$. Standard errors are smaller than the symbol size and omitted for clarity. Lines are guides for the eyes.

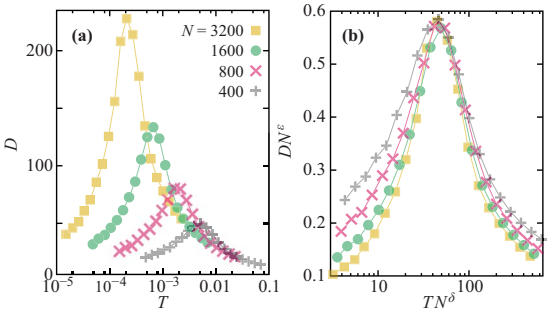

FIG. 4. (Color online) (a) Scaling of the diameter of the largest connected cluster D as a function of temperature and (b) the determination of D's scaling parameters δ and ϵ. We find $\delta=1.52\pm0.02$ and $\epsilon=-0.74\pm0.02$. Standard errors are smaller than the symbol size and omitted for clarity. Lines are guides for the eyes.

case, s_2 gives a strong signal of the low-temperature fragmentation. The heights of the peaks are quite independent of system size. The location of the peak scales to zero such as $T\sim N^{-\gamma}$, $\gamma=1.44\pm0.02$ (not that this value is different from α). This means that the peak of s_2 goes to zero slower than the onset of fragmentation as seen in s_1.

C. Diameter

The *distance* between i and j is the number of edges in the shortest path between the two nodes. The largest distance in a connected subgraph is the *diameter* D of that subgraph. If the picture from Fig. 1 holds—that at intermediate temperatures, the networks are dominated by stretched-out configurations and at lower temperatures they are fragmented—then the diameter of the largest connected component should have a peak at intermediate temperatures. In Fig. 4(a), we plot the diameter as a function of temperature. Indeed there is a peak moving to zero such as $T\sim N^{-\delta}$, $\delta=1.52\pm0.03$, and increasing in size as $N^{-\epsilon}$, with $\epsilon=-0.74\pm0.02$. For the sizes we test, the peak in D occurs at slightly higher temperatures than the peak in s_2. It also scales slightly faster than the s_2 peak toward zero. The fact that the peak of D scales sublinearly reflects that the intermediate region is a mix of configurations, not all stretched out such as Figs. 1(b) and 1(c). This is of course a fundamental aspect of Hamiltonian models—all configurations have a finite chance of appearing at all temperatures, but their frequencies vary with the temperature. The fact that the peak value of D diverges with N supports the picture of circulant ground states (in the $N\to\infty$ limit). The peak in Fig. 4(b) becomes sharper with larger system sizes, meaning that the increase as TN^{δ} is lowered and gets more dramatic. This observation is in concordance with a $T=0$ phase transition. Our data do, however, not give a very strong support for a critical scaling of D at the sizes we investigate.

D. Density dependence

We perform most of our analyses for $M/N=2$, but will briefly touch on how the scaling depends on the density of

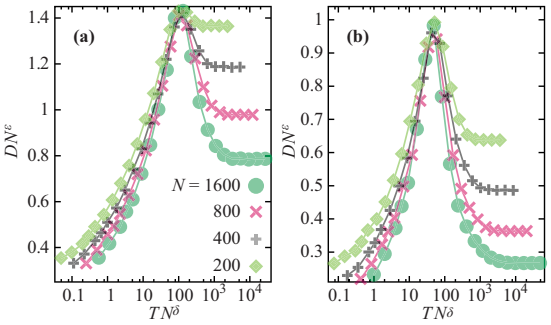

FIG. 5. (Color online) Figures corresponding to Fig. 4(b) for (a) $3N=2M$ and (b) $N=M$. The scaling exponents for (a) are determined to $\delta=1.17\pm0.10$ and $\epsilon=-0.52\pm0.02$; for (b) they are $\delta=1.25\pm0.10$ and $\epsilon=-0.61\pm0.02$. Standard errors are smaller than the symbol size and omitted for clarity. Lines are guides for the eyes.

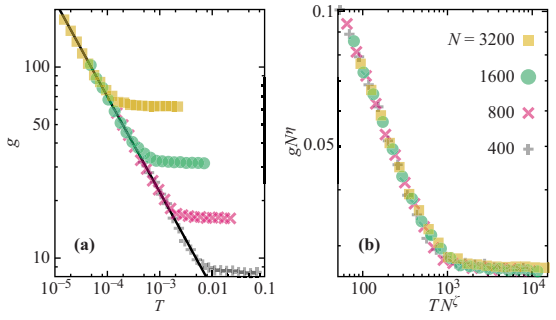

FIG. 6. (Color online) (a) The number of fragments as a function of temperature. The solid line is proportional to $T^{-1/2}$. (b) shows the determination of the scaling exponents $\zeta=1.94\pm0.07$ and $\eta=0.96\pm0.03$. Standard errors are smaller than the symbol size and omitted for clarity.

edges. As our example, we choose the scaling analysis of the diameter seen in Fig. 4(b), but all the other scaling plots give the same conclusion (see Fig. 5). Both the networks with $M/N=2/3$ (a) and $M/N=1$ (b) have peaks of the diameter scaling to zero with increasing sizes. The peak is less marked in the sparser graphs in (a) which is natural since they are closer to the fragmentation threshold at high temperatures ($M/N=1/2$). The exponents are also N dependent, with δ decreasing with decreasing edge density and ϵ increasing (from more to less negative values) as the density becomes larger. If the density is larger, e.g., $M/N=4$, the scaling we plot, at least for the sizes we measure, breaks down (so that there is no δ such that D peaks at the same TN^{δ} and there is no ϵ such that the maximal TN^{ϵ} is the same for all N).

E. Number of isolated subgraphs

Another feature characterizing the fragmentation is the number of connected subgraphs g. In Fig. 6(a), we plot this quantity as a function of temperature. The fragmented and unfragmented states are rather conspicuously separated and in the low-temperature region $g=\Gamma T^{-1/2}$ with the same constant Γ for all system sizes. From Fig. 6(b), we see that

$$g = N^{-\eta} G(TN^{\zeta}), \tag{4}$$

where $\zeta=1.94\pm0.07$, $\eta=0.96\pm0.03$, and G is the function giving the shape seen in Fig. 6(b). In traditional statistical physics, for exactly solvable models, the scaling exponents often have rational values. The g scaling is consistent with a simple picture: if $TN^2 \lesssim 800$, we have $g \sim T^{-1/2}$; if $TN^2 \gtrsim 1600$, we have $g \sim N$. To explain the value of ζ, we note that the energy close to the ground-state energy is governed by angular differences scaling such as $1/N$. Hence, N^{-2} (by the leading, square term of f) gives a local energy scale, which in analogy to van der Waals' law of corresponding states implies that T/N^{-2} is the fundamental quantity for the fragmentation, i.e., that $\zeta=2$. The large TN^{ζ} scaling, $g \sim N$, can be understood from the Erdős-Rényi model that is the high-temperature limit of our YX model and has the same scaling behavior. The low TN^{ζ} scaling, $g \sim T^{-1/2}$, is related to the state with fragmented dense clusters. Assume that all clusters are of similar sizes, then there are N/g vertices in each cluster. The number of edges in a dense cluster scales like $(N/g)^2$ and thus the total number of edges like $M = g(N/g)^2 = N^2/g$. Since we assume sparse graphs, $M \sim N$, the number of clusters in such a graph scales like $g \sim N$. By the same argument as above, that TN^2 is a fundamental quantity, we get $g \sim T^{-1/2}$.

F. Correlations and radial structure

To get a more detailed statistical description of the configurations at different temperatures, we investigate the expectation values ρ of the number of vertices at a distance r from a vertex in Fig. 7. Panels (a) and (b) show the curves below and at the maximum diameter. For these curves, the radial density decreases exponentially, which, we believe, only a fragmentation of the networks can explain. In the $T \to \infty$ limit, the radial density curve looks peaked, as expected in random graphs [31] and similar to observations in large connected networks [32].

In the XY model on two-dimensional lattices, as mentioned, one of the central observations is that the spin correlations decay algebraically in the low-temperature phase as opposed to an exponential decay for high temperatures. In Fig. 8, we graph the correlation function

$$C(r) = |\langle e^{i(\theta_i - \theta_j)} \rangle_r|, \tag{5}$$

where $\langle \cdot \rangle_r$ denotes an average over vertex pair separated by a graph distance r. If all vertex pairs at a certain distance have the same relative angular difference, C will be one. Comparing the four panels, we note that (close to $r=0$) the correlations decay slowest for the lowest temperatures. This is the same behavior as in any classical spin model of statistical physics. But in panels (b) and (c), there is a second peak. We understand this by analogy to the Erdős-Rényi model—if $2M > N$, most vertices of this model are connected into a "giant component," while the rest of the graph consist of small components. In our case, there are also disconnected subgraphs for larger temperatures (i.e., when the graph has a giant component). The nongiant components are sparser than the giant and should therefore be more volatile in structure.

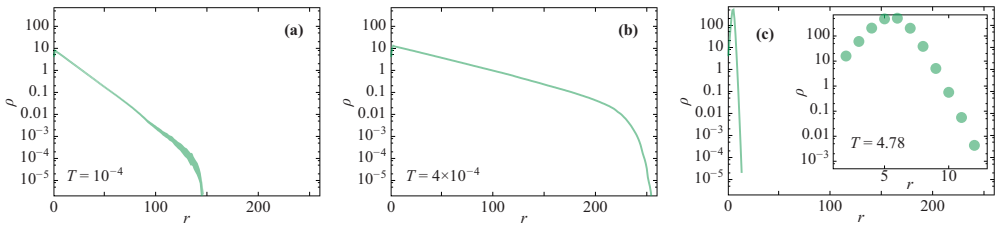

FIG. 7. (Color online) The average density of vertices at a distance r from a vertex for three different temperatures (indicated in the panels) and $N=1600$. To facilitate comparison, we let the panels cover the same ranges. The widths of the lines are at least the standard error. The inset in panel (c) is a blow up.

This leads to lower correlations at distances close to the diameter of the smaller components.

IV. SUMMARY AND DISCUSSION

We have investigated what we call the *YX* model—the *XY* model where the connections, not the spins, are updated—and found a complex pattern of size scaling. There are, for the sizes we study, three regimes: one regime of fragmented configurations dominating at low temperatures, an intermediate-temperature regime dominated by stretched-out networks, and a high-temperature, disordered region. The different quantities we investigate, all capturing different aspects of the network structure, scale to zero with different exponents. Thus the borders between the regimes also scale to zero temperature. For example, we measure the diameter (quantifying how elongated the largest connected component is) and the size of the largest and second-largest components. The peak in diameter scales to $T=0$ like $\sim N^{-1.52\pm0.02}$ while the peak of the size of the second-largest component scales to $T=0$ like $\sim N^{-1.44\pm0.02}$. This multiscaling implies that the picture of three different regions will change as the sizes increase beyond the ones we sample—e.g., the peak of the diameter will, for very large sizes, not coincide with the peak of the size of the second-largest component.

What conclusions can be drawn from our *YX* model as a model of social networks? We have seen that for strong homophily (low temperature), there is a state with stretched-out networks. This regime is shrinking in temperature range as the system size increases. The regime with stretched-out configurations is a "large-world network" in the sense that its distances scale faster than algebraically with N [12]. The fact that this large-world regime vanishes as the system grows is another explanation of the small-world network phenomenon [33] that states that social networks often are very compact in terms of path lengths (usually with distances scaling with the logarithm, or slower, with N). Furthermore, the different scaling exponents we observe suggest that if the system changes in size as it evolves, other network quantities (than the sizes) will change.

In our *YX* model, the role of the $N\to\infty$ limit is, judging from our observations, that regime of fragmented states disappear. There are apparently no emergent singularities. On the other hand, the finite-size scaling shows a complex behavior with different scaling exponents. We cannot rule out a scenario our scaling parameters converge as $N\to\infty$ and there is a unique parameter χ such that all quantities signal the elongated-configuration regime at a critical TN^{χ}. This, we believe, would be the most likely scenario of a phase transition. But nothing in our results suggests this would happen. On the other hand, the size scaling itself is highly complex. Viewed in this way, we have a statistical-physics model where the finite sizes are more interesting than the thermodynamic limit. Moreover, since many real systems (especially in interdisciplinary physics) have restricted sizes, we believe focusing on size scaling rather than extrapolating to infinite sizes is a fruitful future direction for the analysis of statistical-mechanics models.

Our model is disordered and formulated on a statistical-mechanical framework. This forms a common ground with spin-glass models and it would be natural to think that it could be analyzed with the same framework. Spin-glass models are often characterized by some order parameter—a function usually involving sums over all vertices of $F(\theta_i)$ for some function F (typically a trigonometric function to some power). That approach does not work in our case since the set of θ_i's is fixed (so such functions would be constant). One could remedy this by measuring, e.g., the average magnetization per connected component. By such a quantity, one can monitor the fragmentation transition, but it does not contain other information than s_1, s_2, and g. These are the arguments

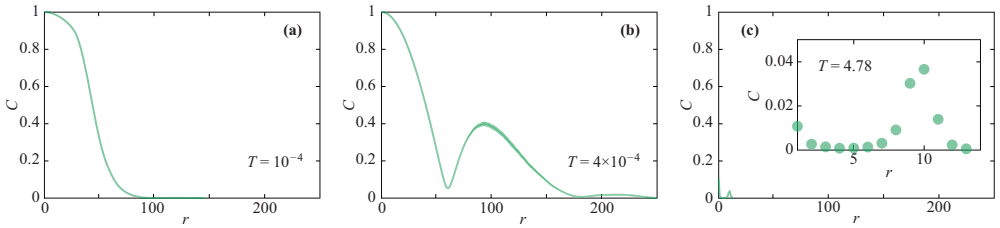

FIG. 8. (Color online) The correlation function as a function of r from for three different temperatures and $N=1600$, plotted in the same way as Fig. 7.

why we mostly focus on network structure of the generated configurations. The only traditional spin-glass measure we use is the correlation function of Fig. 8. The fact that it does not follow any commonly observed functional form, such as exponential or power law, also suggests that our *YX* model needs to be analyzed with a different set of tools. On the other hand, some of our observed phenomena have also been observed in spin glasses. For example, the Heisenberg spin glass with nearest-neighbor interaction in two dimensions also has a $T=0$ transition where the Binder cumulants of spin and chiral order scale to zero with N to the power of different exponents [34]. In sum, we believe spin-glass theory may be helpful to explain some features of our model, but radically new theory is needed as well.

ACKNOWLEDGMENTS

The authors thank Beom Jun Kim for constructive comments. P.H. acknowledges support from the Swedish Foundation for Strategic Research and the WCU (World Class University) program through the Korea Science and Engineering Foundation funded by the Ministry of Education, Science and Technology (Grant No. R31–2008–000–10029–0). Z.X.W. and P.M. acknowledge support from the Swedish Research Council.

[1] M. Suzuki, in *Physics of Low-Dimensional Systems*, edited by Y. Nagaoka and S. Hikami, Proceedings of Kyoto Summer Institute (Publication Office, Progress in Theoretical Physics, Kyoto, 1979), p. 39.
[2] H. Meyer-Ortmanns, Rev. Mod. Phys. **68**, 473 (1996).
[3] J. Toner and Y. Tu, Phys. Rev. Lett. **75**, 4326 (1995).
[4] G. Korniss, M. A. Novotny, H. Guclu, Z. Toroczkai, and P. A. Rikvold, Science **299**, 677 (2003).
[5] J. M. Kosterlitz and D. J. Thouless, J. Phys. C **6**, 1181 (1973).
[6] B. J. Kim, H. Hong, P. Holme, G. S. Jeon, P. Minnhagen, and M. Y. Choi, Phys. Rev. E **64**, 056135 (2001).
[7] K. Medvedyeva, P. Holme, P. Minnhagen, and B. J. Kim, Phys. Rev. E **67**, 036118 (2003).
[8] J.-S. Yang, W. Kwak, K.-I. Goh, and I.-M. Kim, EPL **84**, 36004 (2008).
[9] S. K. Baek, P. Minnhagen, and B. J. Kim, EPL **79**, 26002 (2007).
[10] S. Catterall, J. Kogut, and R. Renken, Nucl. Phys. B **408**, 427 (1993).
[11] R. Albert and A.-L. Barabási, Rev. Mod. Phys. **74**, 47 (2002).
[12] M. E. J. Newman, SIAM Rev. **45**, 167 (2003).
[13] S. N. Dorogovtsev and J. F. F. Mendes, *Evolution of Networks: From Biological Nets to the Internet and WWW* (Oxford University Press, Oxford, 2003).
[14] T. A. B. Snijders, P. E. Pattison, G. L. Robins, and M. S. Handcock, Sociol. Methodol. **36**, 99 (2006).
[15] O. Frank and D. Strauss, J. Am. Stat. Assoc. **81**, 832 (1986).
[16] C. Anderson, S. Wasserman, and B. Crouch, Soc. Networks **21**, 37 (1999).
[17] J. Park and M. E. J. Newman, Phys. Rev. E **70**, 066117 (2004).
[18] G. Caldarelli, A. Capocci, P. De Los Rios, and M. A. Muñoz, Phys. Rev. Lett. **89**, 258702 (2002).
[19] A. E. Motter, T. Nishikawa, and Y.-C. Lai, Phys. Rev. E **68**, 036105 (2003).
[20] D.-H. Kim, B. Kahng, and D. Kim, Eur. Phys. J. B **38**, 305 (2004).
[21] K. Sznajd-Weron and J. Sznajd, Int. J. Mod. Phys. C **11**, 1157 (2000).
[22] J. M. McPherson, Am. Sociol. Rev. **48**, 519 (1983).
[23] P. W. Holland and S. Leinhardt, Am. J. Sociol. **77**, 1205 (1972).
[24] T. C. Schelling, J. Math. Sociol. **1**, 143 (1971).
[25] P. Holme and M. E. J. Newman, Phys. Rev. E **74**, 056108 (2006).
[26] S. Gil and D. H. Zanette, Phys. Lett. A **356**, 89 (2006).
[27] M. E. J. Newman and G. T. Barkema, *Monte Carlo Methods in Statistical Physics* (Oxford University Press, Oxford, 1999).
[28] H. C. White, Am. J. Sociol. **87**, 517 (1981).
[29] G. Bonanno, G. Caldarelli, F. Lillo, and R. N. Mantegna, Phys. Rev. E **68**, 046130 (2003).
[30] K. Hukushima and K. Nemoto, J. Phys. Soc. Jpn. **65**, 1604 (1996).
[31] T. Kalisky, R. Cohen, O. Mokryn, D. Dolev, Y. Shavitt, and S. Havlin, Phys. Rev. E **74**, 066108 (2006).
[32] P. Holme, J. Karlin, and S. Forrest, Proc. R. Soc. London, Ser. A **463**, 1231 (2007).
[33] D. J. Watts and S. H. Strogatz, Nature (London) **393**, 440 (1998).
[34] H. Kawamura and H. Yonehara, J. Phys. A **36**, 10867 (2003).